JCTC Journal of Chemical Theory and Computation

Article

pubs.acs.org/JCTC

Calculating High Energy Charge Transfer States Using Optimally Tuned Range-Separated Hybrid Functionals

Arun K. Manna, Myeong H. Lee,† Kayla L. McMahon, and Barry D. Dunietz*

Department of Chemistry, Kent State University, Kent, Ohio 44242, United States

Supporting Information

ABSTRACT: Recently developed optimally tuned range-separated hybrid (OT-RHS) functionals within time-dependent density functional theory have been shown to address existing limitations in calculating charge transfer excited state energies. The RSH success in improving the calculation of CT states stems from enforcing the correspondence of the frontier molecular orbitals (FMOs) to physical properties, where the highest occupied MO energy relates to the ionization potential and the lowest unoccupied MO energy relates to the electron affinity. However, in this work, we show that a less accurate description of CT states that involves non-FMOs is afforded by the RSH approach. In order to achieve a high quality description of such higher energy CT states, the parameter tuning procedure, which lies at the foundation of the RSH approach, needs to be generalized to consider the CT process. We demonstrate the need for improved description of such CT states in donor−acceptor systems, where the optimal tuning parameter is accounting for the state itself.

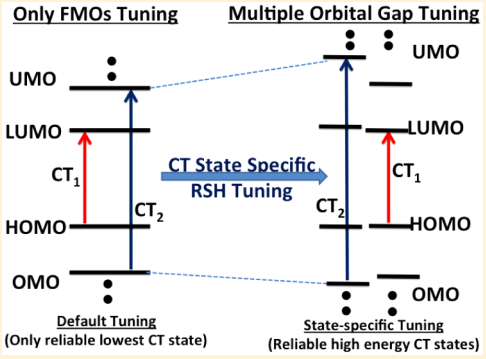

INTRODUCTION

Charge transfer (CT) is the key process in many photochemical reactions in various organic electron donor−acceptor systems, including small organic molecules to organic semiconducting materials, photosynthesized dyes that functionalize inorganic surfaces, large biological pigments, and photosynthetic reaction centers in light-harvesting complexes.[1−20] A molecular level understanding of CT mechanisms in organic semiconducting materials may help to optimize related device performances by shedding light on intrinsic key parameters and means to achieve their tuning. Consequently, CT processes in many interesting electron donor−acceptor systems, including small molecules and extended materials, are at the center of both experimental and theoretical intensive research endeavors.

Computational modeling of the CT processes allows us to understand various photophysical and photochemical processes in detail. Electronic structure calculations of the CT electronic states based on many-body perturbation theory typically within the GW approximation (where G stands for the Green function and W is the dynamically screened Coulomb potential)[21−23] augmented by solving the Bethe−Salpeter equation (BSE) can be used to describe accurately quasi-particle gaps and excitation energies. However, GW-BSE calculations that have been shown to also depend strongly on the details of the implementation[24−28] are computationally demanding and therefore of limited applicability. Thus, developing an alternative scheme to obtain quantitatively accurate descriptions of the fundamental gaps and CT excitation energies, that is, computationally less expensive and more robust, remains highly desirable.

State-of-the-art density functional theory (DFT) and time-dependent DFT (TDDFT) are used extensively to calculate ground and excited state properties of moderate-to-large systems with an accepted level of accuracy and at an affordable computational cost. However, DFT and TDDFT approaches based on standard exchange-correlation (XC) functionals have been shown to underestimate the quasi-particle energy gaps and CT state energies, respectively.[29,30] The source of these artifacts is the improper description of the long-range Coulomb potential by standard XC kernels that have a fixed weight of the local density approximation. Such functionals suffer from a lack in the derivative discontinuity and from many-electron self-interaction error.[31−33] An inclusion of the Hartree−Fock (HF) exchange in the XC functional mitigates only partially these effects when introduced with a fixed weight, as implemented in widely used hybrid functionals (e.g., B3LYP).[34−37]

More recently, long-range corrected (LRC) XC functionals,[38] where the XC potential switches between short-range and long-range expressions at a designated cutoff distance, have been developed and achieved substantially improved quasiparticle energy gaps and CT excitations energies (when used in TDDFT) over traditional functionals with mixing exact and LDA exchange at a prefixed proportion. Correct asymptotic description of the CT state energies (i.e., of $1/R$ dependence) calculated using range-separated hybrid (RSH) functionals is now well established.[38−44] Further improvement is offered by optimally tuning (OT) the range-separation switching parameter. The success of OT RSH functionals relies on the system specific parameter, where accurate fundamental gaps and CT excitations energies are

Received: November 14, 2014

DOI: 10.1021/ct501018n
J. Chem. Theory Comput. XXXX, XXX, XXX−XXX

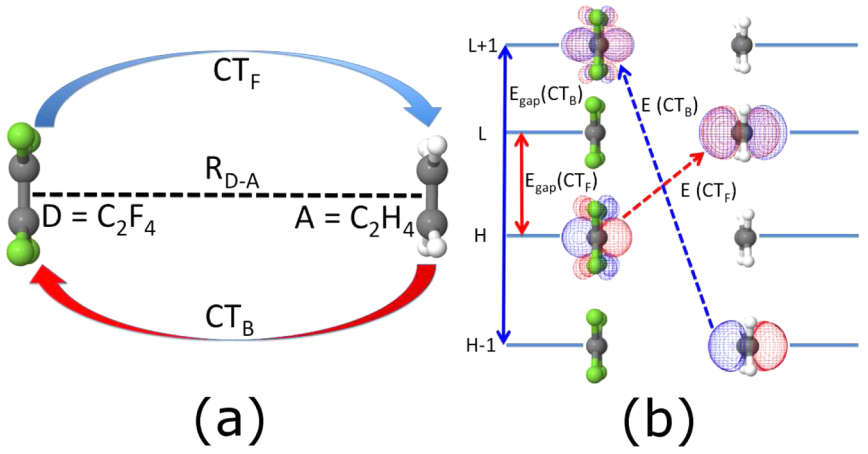

Figure 1. (Color online) (a) CT in C_2F_4–C_2H_4 D–A model system, where forward (low energy) and backward (high energy) transfers are possible. (b) MO diagram illustrating the two CT processes.

produced.[43,45−50] Along with the successes associated with the RSH approach, there are several challenges that are known to limit its applicability and accuracy.[44,51−53] One key aspect is related to the size-consistency of the OT-RSH approach, where the total energy of the system is not guaranteed to be the sum of the total energies of the subunits.[52] This artifact arises from the dependence of the switching parameter on the system size. This problem is especially aggravated when the switching parameter is substantially varied between the two isolated subunits. Below, we show that the heterogeneity may also reflect on the need to retune the RSH when higher energy CT states are considered.

In this study, we examine the accuracy in OT-RSH calculations of excited states that designate the D/A to subunits differently than affected for the lowest CT state. These states involve deeper lying orbitals that are not the system frontier MOs (FMOs), while these orbitals may be FMO of the subunits. Namely, these states energies (E_{CT}) are *not* well associated with the analytical expression $IP^D + EA^A - 1/R$ but rather may involve excited ionization potential (IP) and/or electron affinity (EA). For example the backward transfer process is associated with $E_{CT} \approx IP^A + EA^D - 1/R$, where the roles of the subunits as D/A are reversed. The current OT-RSH functionals enforce physically meaningful frontier HOMO and LUMO that are associated with the IP and EA, respectively, and therefore achieve reliable description of the transfer process involving the FMOs, which typically is associated with the lowest energy CT state.

The main goal of this paper is to show that, for achieving the same high quality description of various CT states within the same system, the tuning in RSH functionals needs to be generalized. In demonstrating the need of tuning per the process, we start by considering a D–A dimer model, where the two directions of CT are considered and then proceed to the various CT states that are present in larger molecular systems within a trimer model involving two D molecules and within a triad molecule. We calculate tuning parameters, where each corresponds to a CT process through enforcing the proper alignment of the relevant orbital gap to the corresponding IP-EA gap.

METHOD: OPTIMALLY TUNED RANGE SEPARATION SWITCHING SCHEME

RSH functionals partition the Coulomb term $(1/r)$ into a short-range functional that determines the localization of the orbitals and a long-range one that sets the asymptotic behavior to follow the exact exchange (Fock-like) and consequently ensures a correct fundamental gap (HOMO–LUMO). Recently, the success of OT-RSH to achieve proper HOMO–LUMO gaps was indicated to stem from the inclusion of the exact exchange by analyzing hyperpolarizabilities of several large CT molecular systems.[53] In the OT-RSH scheme, the Coulomb interaction takes the generalized form:

$$\frac{1}{r} = \frac{\alpha + \beta\ \mathrm{erf}(\gamma r)}{r} + \frac{1 - \alpha - \beta\ \mathrm{erf}(\gamma r)}{r} \quad (1)$$

As widely implemented we set $\alpha + \beta = 1$, where α determines the short-range Fock exchange weight. In the OT-RSH scheme the γ parameter is then varied to enforce correspondence of the HOMO with the IP simultaneously for the system and its ionized states. The separation switching parameter (γ) determines the system dependent distance, where the above exchange functional is replaced by a purely Coulombic electrostatic term. While the α parameter can be determined using first-principles considerations in some cases,[54,55] in practice, it is fixed at a value in the range 0.0–0.3.[56,57] A choice of $\alpha = 0$ corresponds to a pure RSH functional, while $\alpha = 1$ corresponds essentially to a non-RSH functional set to the chosen short-range (SR) XC functional.

We base our OT-RSH approach on the LRC-ωPBEh hybrid functional.[56] The LRC-ωPBEh contains a HF exchange α fraction in the SR exchange term and the rest $(1-\alpha)$ is set by the PBE exchange. We follow previous studies and use $\alpha = 0.20$, which was shown to produce acceptable molecular ground state as well as excited state properties.[54,56] While the amount of SR HF exchange as determined by α may affect the ordering of deeper lying orbitals,[54] we find that the orbital ordering and the fundamental gap are only weakly affected by the α parameter in the considered range of values ([0.0,0.3]; see Supporting Information (SI) Figure 1).

In analyzing the tuning scheme, we refer back to the original J^2 scheme,[43,58] where the HOMO energies of the system in both the donating and accepting forms are associated with corresponding IPs:

DOI: 10.1021/ct501018n
J. Chem. Theory Comput. XXXX, XXX, XXX–XXX

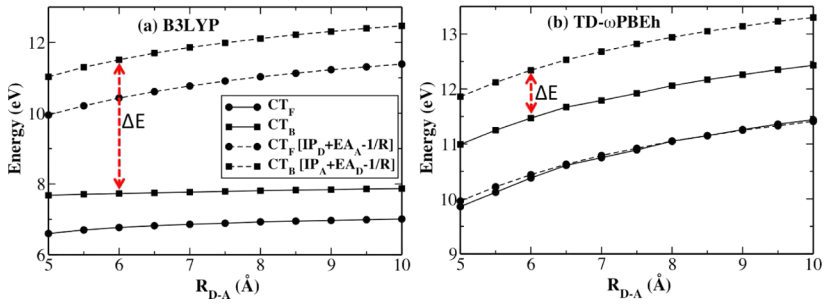

Figure 2. (Color online) Variation of CT state energy along the D−A separation (R_{D-A}) calculated using B3LYP (a) and ωPBEh (b) functionals, where the values due to the corresponding analytical expressions are provided by dotted lines (model system in Figure 1). A quantitative agreement between the analytical and the TDDFT energies is achieved only for the forward process using the RSH functional. The ΔE in the figure highlights the underestimation of the CT_B energy compared to the analytical value, where the error remains substantial using the J^2 scheme (though significantly smaller than the B3LYP error).

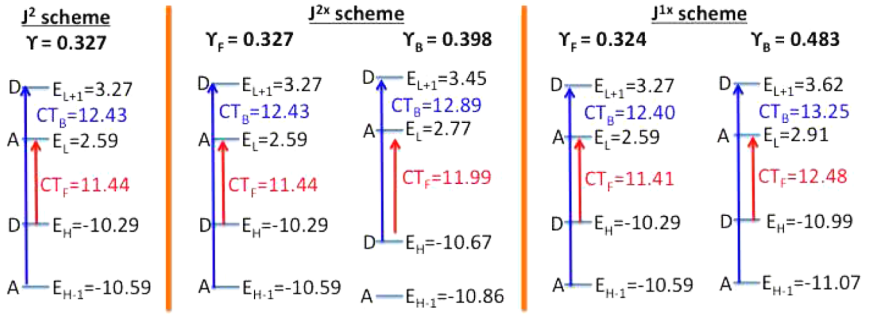

Υ Dependent Monomer's IP and EA and Analytical CT Energies

Υ →	0.324	0.327	0.398	0.483
IP_D; EA_A; CT_F :	10.40; 2.44; 11.40	10.41; 2.44; 11.41	10.50; 2.42; 11.47	10.60; 2.40; 11.56
IP_A; EA_D; CT_B :	10.51; 4.23; 13.30	10.51; 4.23; 13.30	10.46; 4.26; 13.28	10.41; 4.29; 13.26

Figure 3. (Color online) FMO energies at several γ values using the ωPBEh RSH functional with the different tuning schemes for the model D−A at R_{D-A} = 10 Å. Lower panel: The IP and EA values for the D (C_2F_4) and A (C_2H_4) calculated at the different tuning parameters. (Energies are listed in eV.)

$$J^2(\gamma) = [\mathrm{IP}^\gamma(\mathrm{DA}) + \varepsilon_\mathrm{H}^\gamma(\mathrm{DA})]^2 + [\mathrm{IP}^\gamma(\mathrm{DA}^{-1}) + \varepsilon_\mathrm{H}^\gamma(\mathrm{DA}^{-1})]^2 \quad (2)$$

Alternatively, the J error measure can be defined by considering the HOMO and LUMO of the DA system relative to their IP and EA, respectively:[45,58]

$$J^{2'}(\gamma) = [\mathrm{IP}^\gamma(\mathrm{DA}) + \varepsilon_\mathrm{H}^\gamma(\mathrm{DA})]^2 + [\mathrm{EA}^\gamma(\mathrm{DA}) + \varepsilon_\mathrm{L}^\gamma(\mathrm{DA})]^2 \quad (3)$$

(We follow: EA ≡ $E(\mathrm{DA}) - E(\mathrm{DA}^{-1})$; IP ≡ $E(\mathrm{DA}^{+1}) - E(\mathrm{DA})$). Both the J^2 and $J^{2'}$ error measures are found to be practically equivalent, reflecting a minimized discontinuity in the exchange functional.[45] By minimizing these J^2 error measures the curvature of the chemical potential is minimized at integer electron occupations reinforcing the piecewise linearity of the energy with respect to the electron count. In this way, the underestimation of the IP and EA by the FMO energies is minimized.[51,54,58−61] Below, we use the J^2 measure for benchmarking and the $J^{2'}$ expression to derive new error measures that are applicable to address high-energy CT states with greater accuracy.

Ground state monomer geometries are optimized using B3LYP[34−37] hybrid functional with cc-pVTZ basis set for all atoms. Excited states calculations are carried out at TDDFT/ωPBEh level using cc-pVTZ basis set for all atoms. All calculations reported here are implemented using Q-Chem version 4.1.[62,63]

Tuning for Backward and Forward CT States in a Model D−A Dimer. We start our analysis of the need to retune for each CT state by considering a weakly coupled D−A model system, where C_2F_4 is the D and C_2H_4 is the A. This D−A pair served as a benchmark model system to identify the fundamental limitations in CT modeling using conventional DFT.[64] At sufficiently large distances the D and A regions are weakly coupled and therefore are associated with complete electron transfer states. A diagram of the relevant FMOs is shown in Figure 1, where we also illustrate the forward and backward CT states involving these orbitals. Here, the high-energy CT state corresponds to the backward transfer direction, where the molecules switch their roles as the D and A of the charge in the process.

The distance dependence energies of both CT states are shown in Figure 2. We point out the well-documented failures of functionals that involve a fixed amount of the local density approximation where CT states energies are underestimated and are independent of the distance (R) instead of following the expected $1/R$ trend (the B3LYP is used as an example).

DOI: 10.1021/ct501018n
J. Chem. Theory Comput. XXXX, XXX, XXX−XXX

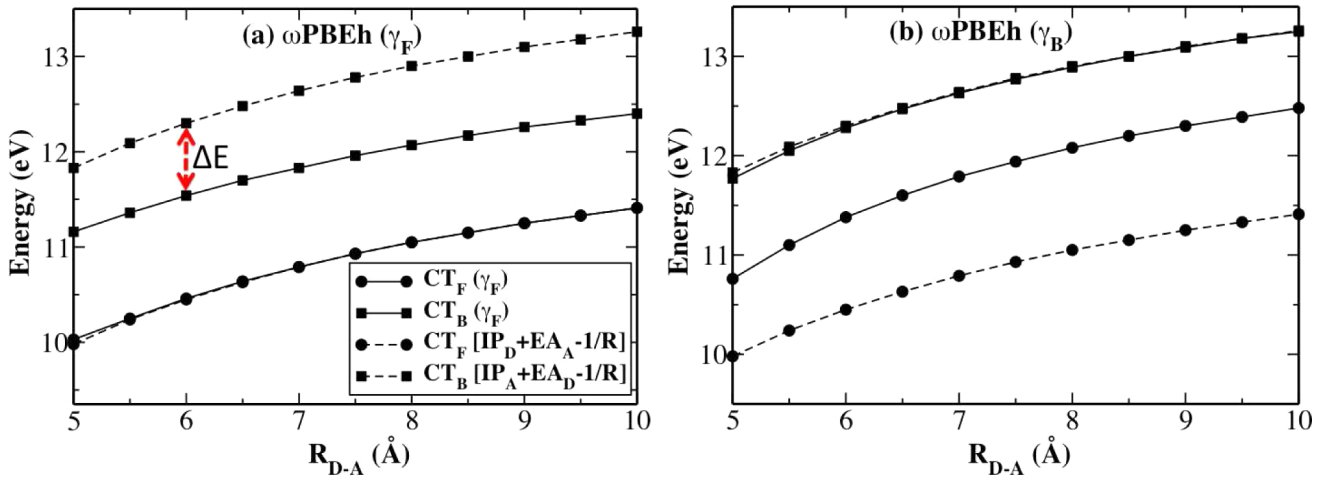

Figure 4. (Color online) Variation of the CT state energy along the D−A separation calculated using RSH ωPBEh functional tuned using the J^{1x} with the (a) forward parameter (J^{1F}) (b) backward parameter (J^{1B}). The values due to the corresponding analytical expressions are provided by dotted lines. A quantitative agreement between the analytical energy and the TDDFT energy for the backward process is achieved for the RSH functional tuned by the relevant J^{1B} scheme (in addition to the expected agreement for the forward process when J^{1F} is used). The substantial underestimation of the CT_B when using the J^{1F}-based parameter is highlighted by the ΔE.

Though, recently, the success of OT-RSH to achieve proper HOMO−LUMO gaps was indicated to stem from the substantial inclusion of the exact exchange by analyzing hyperpolarizabilities of several large CT molecular systems.[53] We confirm the success of the RSH ωPBEh functional in correcting these anomalies when considering the lowest (forward) CT state (CT_F). However, the backward CT state energy is greatly underestimated by the RSH ωPBEh functional in comparison to the analytical benchmark value, while reproducing the proper $1/R$ dependence. We have employed the widely used J^2 scheme for tuning the range separation parameter (see eq 2). The parameter values at different distances are provided in SI Table 1.

In systems involving well-separated D and A subunits, the $J^{2'}$ scheme can be modified to use IP/EA values of the monomers. The resulting J^{2x} scheme involves the following error measure

$$J^{2x}(\gamma;\alpha) = [\mathrm{IP}^{\gamma;\alpha}(\mathrm{D}_x) + \varepsilon^{\gamma;\alpha}_{\mathrm{H}_{\mathrm{D}x}}(\mathrm{DA})]^2 + [\mathrm{EA}^{\gamma;\alpha}(\mathrm{A}_x) + \varepsilon^{\gamma;\alpha}_{\mathrm{L}_{\mathrm{A}x}}(\mathrm{DA})]^2 \quad (4)$$

(where a designation of the donor/acceptor subunits is indicated by x. Here, this designation can switch between the two transfer directions (forward [x = F] and backward [x = B]). Therefore, with $\varepsilon^{\gamma;\alpha}_{\mathrm{H}_{\mathrm{D}x}}$ for x = F (or B), we refer to the HOMO (HOMO − 1) orbital within the DA coupled system, which is localized on the designated donor region (D is the actual proper donor for x = F, but D is set to the acceptor for the x = B case). We emphasize that in the limit of vanishing D−A coupling the Janak theorem (DFT equivalent theorem to Koopman's theorem) holds simultaneously for both the D and the A units. Therefore, at that limit the J^{2x} measure is justifiable for the backward CT process as it is for the forward transfer case.

The different γ values for the forward and backward processes that follow the J^{2x} expressions ($J^{2F}(\gamma)$ and $J^{2B}(\gamma)$, respectively) are provided in Figure 3. For the forward CT case, the γ value remains essentially the same (γ_{J^2} = 0.327 and $\gamma_{J^{2F}}$ = 0.327 [Formally, γ_{J^2} and $\gamma_{J^{2F}}$ can be different since the HOMO in the DA system, which is localized on the D can be different than the HOMO of the isolated D]). On the other hand, the $\gamma_{J^{2B}}$ value of 0.398 indicates a significantly affected parameter by the switched D/A designation. We also provide the FMOs energies at the different γ values and the CT state energies calculated using TDDFT with the varied parameter. The forward CT energy corresponds well within 0.1 eV of the analytical value following the J^2 scheme (and J^{2x}). The backward CT energy, on the other hand, is underestimated by 0.9 eV when using the J^2 parameter, where the error while significantly reduced remains high at 0.4 eV using the J^{2x} parameter. The remaining error by the J^{2x} scheme in calculating the backward state stems from the difficulty in aligning non FMOs to IP energies, since such correspondence is not warranted.

The auspicious J^2 scheme is based on enforcing simultaneously correspondence of the HOMO and LUMO with the IP and EA energies respectively, thereby achieving the proper treatment of the lowest CT state in TDDFT. However, in higher CT states deeper MOs (not the FMOs) are involved. The early RSH scheme (J^1)[40,43] enforces correspondence only between the IP and HOMO of the coupled system and therefore achieved only a moderate success (subsequently improved by J^2), while providing a step forward over conventional DFT. Here, we generalize the tuning to consider the specific CT state. In considering a specific CT process, the J^{1x} scheme aligns the relevant orbital gap (occupied to unoccupied MOs: OMO-UMO) to the corresponding |EA-IP| gap:

$$J^{1x}(\gamma;\alpha) = |\mathrm{IP}^{\gamma;\alpha}(\mathrm{D}x) - \mathrm{EA}^{\gamma;\alpha}(\mathrm{A}x)| - |\varepsilon^{\gamma;\alpha}_{\mathrm{H}_{\mathrm{D}x}}(\mathrm{DA}) - \varepsilon^{\gamma;\alpha}_{\mathrm{L}_{\mathrm{A}x}}(\mathrm{DA})| \quad (5)$$

In this way, we guarantee that the Cassida expression for the high energy CT excitations utilizes physically meaningful orbital gaps. The γ of the backward process can be found by switching the roles of the donor and acceptor subunits. We use the modified J^{1x} that directly aligns the relevant gaps to demonstrate the difference in the optimal switching parameters for the various CT states within the same system.

The importance of retuning for each state is indicated by the difference between the γ values evaluated using the J^{1F} and J^{1B} schemes, where they are are found to be 0.324 and 0.483.

DOI: 10.1021/ct501018n
J. Chem. Theory Comput. XXXX, XXX, XXX−XXX

Namely, the forward value (due to J^{1F}) is similar to the default parameter (0.327, due to J^2), whereas the parameter (due to J^{1B}) is significantly different (increased) for the backward process. The backward and forward CT energies are confirmed to be within 0.1 eV of the analytical values when using the corresponding J^{1x}-based parameters as expected from the direct tuning. The success in the fitting of the relevant gaps of the forward and backward transfer processes by using the J^{1x} parameters is well demonstrated. The distance dependence of the CT states calculated using the various parameters is compared to the analytical expression in Figure 4. The error (ΔE) in calculating the backward CT energy, when the same default parameter is used (i.e., following the J^2 scheme), is shown by the red arrow.

Multiple CT States in $H_2PC-H_2PC-C_{60}$ D−D−A Complex. The copper phthalocyanine (CuPC)−fullerene D−A heterojunction is a widely studied model organic photovoltaic system.[65−72] We next consider a related D−D−A trimer model consisting of a pair of metal-free phthalocyanine (the D) and a single C_{60} (the A), see Figure 5. Recently, we have studied the role of a variety of CT states in a similar D−D−A trimer model system. The excited states of the trimer (D_2-D_1-A) model can be categorized into four groups:

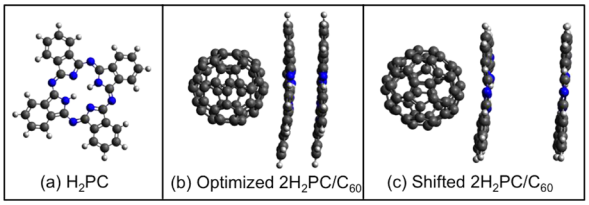

	$E_{TDDFT/\omega PBEh}(\gamma_{J^2})$	$E_{TDDFT/\omega PBEh}(\gamma_{J^1})$	$E_{TDDFT/B3LYP}$
π-π^*	2.26 (0.113)	2.26	2.23
αCT	1.96 (0.113)	2.01 (0.123)	1.59
$ddCT_1$	2.46 (0.113)	2.59 (0.131)	1.83
$ddCT_2$	2.60 (0.113)	2.67 (0.122)	1.90
βCT	2.90 (0.113)	3.06 (0.130)	1.69

Figure 5. Vertical excitation energy in eV, in parentheses the range-separation parameter (γ) in $bohr^{-1}$ using the J^2 and J^{1x} tuning schemes. The γ value for the EX state is not shown for the J^{1x} tuning scheme because the EX state energy remains the same regardless of the γ value. Last column shows the excitation energies using the B3LYP functional.

- Bright donor-localized $\pi-\pi^*$ states ($(D_2D_1)^*A$), which we denote EX.
- Dark nearest-neighbor donor-to-acceptor CT states ($D_2D_1^+A^-$), which we denote αCT.
- Dark second-nearest-neighbor donor-to-acceptor CT states ($D_2^+D_1A^-$), which we denote βCT.
- Dark donor-to-donor CT states ($D_2^+D_1^-A$ and $D_2^-D_1^+A$), which we denote $ddCT_1$ and $ddCT_2$, respectively.

The βCT states are hot CT states of decreased exciton binding energy and increased transfer distance than in the αCT (cold CT) states of the shorter range. In ddCT states, the transfer occurs between the two donors (H_2PCs), and it arises from their broken symmetry induced by the C_{60}.

We obtain the ground-state equilibrium geometry using the ωB97X-D dispersion-corrected functional to address the noncovalent interactions.[73,74] To account for the effect of the solid state environment in thin films, we employ a polarizable continuum model (PCM)[75] with a dielectric constant 4.2,[70,76−81] when performing the geometry optimization. We then proceed to calculate the CT properties, where the distance between the monomers is increased by 4 Å to ensure full electron transfers within the different CT states. A similar approach has been used by us to provide the electronic structure parameters for calculating the rates of photoinduced CT processes in organic semiconducting materials.[72,82−84] In this model, we find the FMOs (and those next to them) to be localized on a subunit, where HOMO and LUMO+4 are localized on D_2, and HOMO−1 and LUMO+3 are localized on D_1, and the LUMO, LUMO+1 and LUMO+2 are localized on the C_{60}.

The vertical excitation energies obtained using TDDFT/ωPBEh with γ values optimized following the $J^2(\gamma)$ and $J^{1x}(\gamma)$ tuning schemes and using TDDFT/B3LYP are shown in Figure 5. (The lowest excited state of each group is presented.) While the EX state energy level changes only slightly between using the different functionals, the RSH CT states energies are all higher than the B3LYP values. All CT states are of one electron transfer. The orbitals involved in the CT excitations are illustrated in the SI Figure 2.

The CT states energies while sensitive to the switching parameter value, maintain the same ordering of the states with all calculated parameters ($E_{\alpha CT} < E_{EX} < E_{ddCT_1} < E_{ddCT_2} < E_{\beta CT}$). In all cases the J^{1x} parameter is larger than the J^2 parameter, reflecting a shorter switching distance resulting with increase in

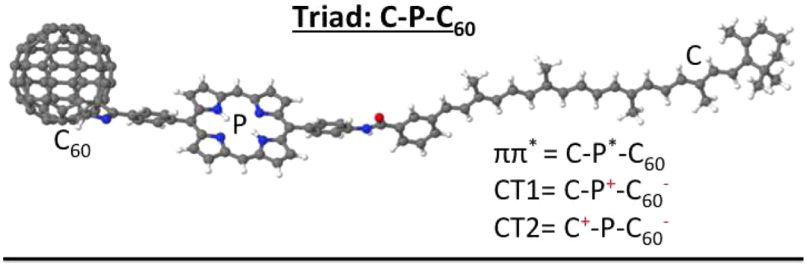

Electronic State	TDDFT/OT-RSH-ωPBEh/γ_{CT1}= 0.127 Excitation Energy (eV)	ΔQ (e)	TDDFT/ OT-RSH-ωPBEh/γ_{CT2}=0.120 Excitation Energy (eV)	ΔQ (e)
ππ*	2.24 (0.087)	0.00	2.24 (0.093)	0.00
CT1	**2.62 (0.001)**	**0.99**	2.55 (0.000)	0.98
CT2	2.70 (0.000)	1.00	**2.61 (0.000)**	**1.00**

Figure 6. (Color online) Molecular structure of the C−P−C_{60} molecular triad. The excited state energies with oscillator strengths in parentheses and the amounts of charge separation (ΔQ) are listed in the tabular insert (lower panel).

DOI: 10.1021/ct501018n
J. Chem. Theory Comput. XXXX, XXX, XXX−XXX

CT energies. The CT state energies increase when employing the $J^{1x}(\gamma)$ tuning scheme by 0.05 eV (αCT), 0.13 eV ($ddCT_1$), 0.07 eV ($ddCT_2$), and 0.16 eV (βCT). The increase of the excitation energy is most pronounced for the (hot) βCT state which is also the longest range process, while the overall energetic effect is substantially smaller than found for the dimer model system considered above. Systems with even weaker coupled D/A units or greater difference in the fundamental gap alignment may lead to increased energetic effect due to the retuning.

Multiple CT States in a Molecular Triad (C−P−C_{60}). We next consider a complicated coupled D−A system involving three chromophores forming a D−B−A triad, where B corresponds to a bridge that can participate either as a donor or as an acceptor in a CT process. Specifically, we consider a D−B−A triad of carotene polyene (C) [D], diaryl porphyrin (P) [B], and carbon fullerene (C_{60}) [A], referred to as C−P−C_{60}. This system has been widely studied due to its potential use in light-harvesting and photonics applications.[6,11,14,85−88] The triad C−P−C_{60} contains two D units (C and P) and one A unit (C_{60}) that are bonded and are relatively strongly coupled unlike the D−A systems discussed above.

Experimental as well as previous theoretical studies[85−87] confirm the presence of two different CT excited states. The CT state with C_{60} as the A and P as the D is represented by CT1, possessing a relatively small dipole moment. The CT state with C as the D and C_{60} as the A is represented by CT2 possesses a larger dipole moment.

The triad geometry optimized by combining DFT employing B3LYP/SV and a PCM[89] using switching Gaussians for surface discretization[90,91] with a dielectric constant corresponding to the tetrahydrofuran (THF) solvent is shown in Figure 6. We employ the J^{1x} RSH tuning protocol considering the relevant molecular orbitals for each CT process. The resulting γ parameters and excitations energies are listed in Figure 6. The orbitals participating in the CT process are illustrated in SI Figure 3.

The J^{1x} tuning protocol finds two range-separation parameters for the CT states: $\gamma_{CT1} = 0.127$ and $\gamma_{CT2} = 0.120$. The validity of these two γ values is confirmed by comparing to relevant J^2 tuning values. The CT2 of the triad is the lowest energy CT state involving the HOMO−LUMO and therefore the J^{1x}-based parameter for CT2 is expected to be similar in value to the triad's default J^2 value. Similarly, the CT1 of the triad involves the HOMO−LUMO in a B−A dyad, and therefore, the triad's J^{1x} parameter for CT1 should correspond well to the default J^2 parameter of the B−A dyad. Indeed, we find in comparing the optimal γ values that $J^{1x}\gamma_{CT2}(\text{triad}) = J^2\gamma_{CT2}(\text{triad})$ and $J^{1x}\gamma_{CT1}(\text{triad}) = J^2\gamma_{CT}(\text{dyad})$. In calculating the J^2 dyad parameters, we used the IP/EA of the designated D/A unit extracted from the triad model following hydrogen passivation of dangling bonds.

The porphyrin absorbing state $\pi-\pi^*$ energy is only slightly affected by the varying switching parameter value (within 0.01 eV). While the CT states energies are more affected within the range of 0.07−0.09 eV. The CT1 and CT2 state energies using γ_{CT1} are 2.62 and 2.70 eV, respectively, and 2.55 and 2.61 eV using the range-separation parameter γ_{CT2} (see tabulated data in Figure 6). The CT1 (CT2) state energy is underestimated (overestimated) by about 0.07 eV (0.09 eV) when using the wrong range-separation parameter in TDDFT/ωPBEh calculations. The CT energies using optimal parameters per state are 2.62 eV for the CT1 state and 2.61 eV for the CT2 state (see the listed data in bold letters in Figure 6). Both CT states, in the considered geometry, involve a single electron being transferred in spite of the chemical bonding of the triad subunits. The amount of charge transfer is evaluated comparing the Mulliken atomic charges of the relevant subunits between the excited state and the ground state. We do not find variation in transferred charge (ΔQ) when using the different γ parameters.

The overall energetic effect due to retuning is relatively small (smaller than 0.1 eV also for the trimer model above), which is within acceptable chemical accuracy. Though, by using the retuning-corrected J^{1x} CT state energies in modeling CT rates, we find a trend of improved agreement with measured values. The relatively large changes of the rate constant reflect the strong dependence of the rate expression on the energy parameters. In a recent study, the measured rate of a photoinduced process in the triad was associated with the CT1 process,[92] where a J^2 tuning scheme was employed in calculating the CT state energy. The resulting calculated rate was overestimated (1.0×10^{12} s^{-1}) compared to the measured experimental value (3.3×10^{11} s^{-1}).[85] Here, by correcting the CT1 excitation energy using the J^{1x} scheme of a 0.07 eV increase, the calculated rate following Marcus picture (7.1×10^{11} s^{-1}) becomes closer to the experimental value. In providing the rate estimates, we assume that the solvent effects (geometry and energetic stabilization) remain unaffected by the retuning.

CONCLUSIONS

To conclude, we demonstrate the need for adapting the optimal tuning scheme in RSH functionals to the CT state, where the current state-of-the-art implementations of OT RSH is to use the same parameter in calculating all the CT states within the same geometry. The present study highlights the need for adjusting the tuning in OT-RSH functionals to achieve quantitatively correct CT state energies, especially when the system involves various subunits to establish alternative CT processes. We used a J^{1x} tuning scheme that essentially aligns the relevant orbital gap to the corresponding fundamental gap to find the optimal parameter for each process. We used a D−A model system to confirm our approach by comparing against energies calculated using an analytical expression. We then implemented the retuning concept to two complex molecular systems. The two systems include a trimer model relevant to organic photovoltaic systems and a molecular triad that is widely studied for photoinduced CT kinetics. We have found the effect on CT state energies in these larger molecular systems to be relatively small. Further research is needed to quantify the need for retuning. A criterion to require retuning can be based on differences in the optimal switching parameters of the relevant subunits.[52] We used a PBE-based range-separated density functional, with asymptotically exact and short-range fractional Fock exchange but suggest that similar findings are expected for any choice of the RSH protocol.

ASSOCIATED CONTENT

Supporting Information

Model D−A system: Table of TD-ωPBEh calculated CT energies and the range-separation parameters at varying D−A distances. Figure of the Frontier molecular orbital energies with varying α (increasing short-range Fock exchange) and γ range-separation parameters. Triad and trimer models: Figures of the molecular orbitals relevant to the CT excited states. This

DOI: 10.1021/ct501018n
J. Chem. Theory Comput. XXXX, XXX, XXX−XXX

material is available free of charge via the Internet at http://pubs.acs.org/.

AUTHOR INFORMATION

Corresponding Author

*E-mail: bdunietz@kent.edu.

Present Address

†Department of Chemistry and Centre of Scientific Computing, University of Warwick, Coventry CV4 7AL, United Kingdom.

Notes

The authors declare no competing financial interest.

ACKNOWLEDGMENTS

B.D.D. gratefully acknowledges support by a Department of Energy Basic Energy Sciences (DOE-BES) award through the Chemical Sciences Geosciences and Biosciences Division (DE-SC0004924), DE-FG02-10ER16174. We are also thankful to the Ohio Supercomputer and the Kent State University College of Arts and Sciences for making computing resources available to complete the reported research. K.L.M. contributed to the research report here through a summer undergraduate internship. B.D.D. and K.L.M. thank the National Science Foundation for funding of the NSF-REU Program (CHE-1263087).

REFERENCES

(1) Dou, L.; You, J.; Yang, J.; Chen, C.-C.; He, Y.; Murase, S.; Moriarty, T.; Emery, K.; Li, G.; Yang, Y. *Nat. Photonics* **2012**, *6*, 180−185.

(2) Marcus, R. A. *Rev. Mod. Phys.* **1993**, *65*, 599−610.

(3) Nan, G.; Yang, X.; Wang, L.; Shuai, Z.; Zhao, Y. *Phys. Rev. B* **2009**, *79*, 115203.

(4) Yin, S.; Li, L.; Yang, Y.; Reimers, J. R. *J. Phys. Chem. C* **2012**, *116*, 14826.

(5) Troisi, A.; Orlandi, G. *Phys. Rev. Lett.* **2006**, *96*, 086601.

(6) Balamurugan, D.; Aquino, A. J.; de Dios, F.; Flores, L., Jr; Lischka, H.; Cheung, M. S. *J. Phys. Chem. B* **2013**, *117*, 12065−12075.

(7) Yamaguchi, Y.; Yokoyama, S.; Mashiko, S. *J. Chem. Phys.* **2002**, *116*, 6541−6548.

(8) Kobayashi, R.; Amos, R. D. *Chem. Phys. Lett.* **2006**, *420*, 106−109.

(9) Thompson, A.; Ahn, T.-S.; Justin, K. R.; Thayumanavan, T. S.; Martínez, T. J.; Bardeen, C. J. *J. Am. Chem. Soc.* **2005**, *127*, 16348−16349.

(10) Jailaubekov, A. E.; Willard, A. P.; Tritsch, J. R.; Chan, W. L.; Sai, N.; Gearba, R.; Kaake, L. G.; Williams, K. J.; Leung, K.; Rossky, P.; Zhu, X. Y. *Nat. Mater.* **2013**, *12*, 66−73.

(11) Liddell, P. A.; Kuciauskas, D.; Sumida, J. P.; Nash, B.; Nguyen, D.; Moore, A. L.; Moore, T. A.; Gust, D. *J. Am. Chem. Soc.* **1997**, *119*, 1400−1405.

(12) Liddell, P. A.; Kodis, G.; Moore, A. L.; Moore, T. A.; Gust, D. *J. Am. Chem. Soc.* **2002**, *124*, 7668−7669.

(13) Green, M. A. *Third Generation Photovoltaics*; Springer-Verlag: New York, 2003.

(14) Rizzi, A. C.; van Gastel, M.; Liddell, P. A.; Palacios, R. E.; Moore, G. F.; Kodis, G.; Moore, A. L.; Moore, T. A.; Gust, D.; Braslavsky, S. E. *J. Phys. Chem. A* **2008**, *112*, 4215−4223.

(15) Tian, H.; Yu, Z.; Hagfeldt, A.; Kloo, L.; Sun, L. *J. Am. Chem. Soc.* **2011**, *133*, 9413−9422.

(16) Mishra, A.; Fischer, M. K. R.; Bäuerle, P. *Angew. Chem., Int. Ed.* **2009**, *48*, 2474−2499.

(17) Feldt, S. M.; Gibson, E. A.; Gabrielsson, E.; Sun, L.; Boschloo, G.; Hagfeldt, A. *J. Am. Chem. Soc.* **2010**, *132*, 16714−16724.

(18) Giebink, N. C.; Wiederrecht, G. P.; Wasielewski, M. R.; Forrest, S. R. *Phys. Rev. B* **2010**, *82*, 155305.

(19) Giebink, N. C.; Wiederrecht, G. P.; Wasielewski, M. R.; Forrest, S. R. *Phys. Rev. B* **2011**, *83*, 195326.

(20) Zhao, Y.; Liang, W. *Chem. Soc. Rev.* **2012**, *41*, 1075−1087.

(21) Hedin, L. *Phys. Rep.* **1965**, *139*, A796−A823.

(22) Hybertsen, M. S.; Louie, S. G. *Phys. Rev. B* **1986**, *34*, 5390−5413.

(23) Onida, G.; Reining, L.; Rubio, A. *Rev. Mod. Phys.* **2002**, *74*, 601−659.

(24) Grossman, J.; Rohlfing, M.; Mitas, L.; Louie, S.; Cohen, M. *Phys. Rev. Lett.* **2001**, *86*, 472.

(25) Blase, X.; Attaccalite, C.; Olevano, V. *Phys. Rev. B* **2011**, *83*, 115103.

(26) Blase, X.; Attaccalite, C. *Appl. Phys. Lett.* **2011**, *99*, 171909.

(27) Qian, X.; Umari, P.; Marzari, N. *Phys. Rev. B* **2011**, *84*, 075103.

(28) Sharifzadeh, S.; Biller, A.; Kronik, L.; Neaton, J. B. *Phys. Rev. A* **2012**, *85*, 125307.

(29) Dreuw, A.; Head-Gordon, M. *J. Am. Chem. Soc.* **2004**, *126*, 4007−4016.

(30) Wong, B. M.; Hsieh, T. H. *J. Chem. Theor. Comput.* **2010**, *6*, 3704−3712.

(31) Qian, Z.; Sahni, V. *Phys. Rev. B* **2000**, *62*, 16364−16369.

(32) Yang, W.; Cohen, A. J.; Mori-Sanchez, P. *J. Chem. Phys.* **2012**, *136*, 204111−204123.

(33) Mori-Sanchez, P.; Cohen, A. J.; Yang, W. *J. Chem. Phys.* **2006**, *125*, 201102−201105.

(34) Becke, A. D. *J. Chem. Phys.* **1993**, *98*, 5648.

(35) Lee, C.; Yang, W.; Parr, R. G. *Phys. Rev. B* **1988**, *37*, 785−789.

(36) Stephens, P.; Devlin, F.; Chabalowski, C.; Frisch, M. *J. Phys. Chem.* **1994**, *98*, 11623−11627.

(37) Vosko, S.; Wilk, L.; Nusair, M. *Canadian J. Phys.* **1980**, *58*, 1200−1211.

(38) Yanai, T.; Tew, D. P.; Handy, N. C. *Chem. Phys. Lett.* **2004**, *393*, 51−57.

(39) Baer, R.; Neuhauser, D. *Phys. Rev. Lett.* **2005**, *94*, 043002.

(40) Livshits, E.; Baer, R. *Phys. Chem. Chem. Phys.* **2007**, *9*, 2932−41.

(41) Henderson, T. M.; Janesko, B. G.; Scuseria, G. E. *J. Chem. Phys.* **2008**, *128*, 194105−194113.

(42) Kümmel, S.; Kronik, L. *Rev. Mod. Phys.* **2008**, *80*, 3−60.

(43) Stein, T.; Kronik, L.; Baer, R. *J. Am. Chem. Soc.* **2009**, *131*, 2818.

(44) Autschbach, J. *ChemPhysChem* **2009**, *10*, 1757−1760.

(45) Stein, T.; Kronik, L.; Baer, R. *J. Chem. Phys.* **2009**, *131*, 244119.

(46) Zheng, S.; Phillips, H.; Geva, E.; Dunietz, B. D. *J. Am. Chem. Soc.* **2012**, *134*, 6944−6947.

(47) Phillips, H.; Zheng, S.; Hyla, A.; Laine, R.; Goodson, T., III; Geva, E.; Dunietz, B. D. *J. Phys. Chem. A* **2012**, *116*, 1137.

(48) Phillips, H.; Geva, E.; Dunietz, B. D. *J. Chem. Theor. Comput.* **2012**, *8*, 2661−2668.

(49) Zheng, S.; Geva, E.; Dunietz, B. D. *J. Chem. Theor. Comput.* **2013**, *9*, 1125−1131.

(50) Phillips, H.; Zheng, Z.; Geva, E.; Dunietz, B. D. *Opt. Elec.* **2014**, *15*, 1509−1520.

(51) Kronik, L.; Stein, T.; Refaely-Abramson, S.; Baer, R. *J. Chem. Theor. Comput.* **2012**, *8*, 1515−1531.

(52) Karolewski, A.; Kronik, L.; Kümmel, S. *J. Chem. Phys.* **2013**, *138*, 204115.

(53) Garza, A. J.; Wazzan, N. A.; Asiri, A. M.; Scuseria, G. E. *J. Phys. Chem. A* **2014**, *118*, 11787−11796.

(54) Refaely-Abramson, S.; Sharifzadeh, S.; Govind, N.; Autschbach, J.; Neaton, J. B.; Baer, R.; Kronik, L. *Phys. Rev. Lett.* **2012**, *109*, 226405−226408.

(55) Srebro, M.; Autschbach, J. *J. Phys. Chem. Lett.* **2012**, *3*, 576−581.

(56) Rohrdanz, M. A.; Martins, K. M.; Herbert, J. M. *J. Chem. Phys.* **2009**, *130*, 054112−054119.

(57) Vydrov, O. A.; Scuseria, G. E. *J. Chem. Phys.* **2006**, *125*, 234109−234117.

(58) Stein, T.; Eisenberg, H.; Kronik, L.; Baer, R. *Phys. Rev. Lett.* **2010**, *105*, 266802.

(59) Refaely-Abramson, S.; Baer, R.; Kronik, L. *Phys. Rev. B* **2011**, *84*, 075144.

DOI: 10.1021/ct501018n
J. Chem. Theory Comput. XXXX, XXX, XXX−XXX

(60) Stein, T.; Autschbach, J.; Govind, N.; Kronik, L.; Baer, R. *J. Phys. Chem. Lett.* **2012**, *3*, 3740−3744.
(61) Refaely-Abramson, S.; Sharifzadeh, S.; Jain, M.; Baer, R.; Neaton, J. B.; Kronik, L. *Phys. Rev. B* **2013**, *88*, 081204(R).
(62) Shao, Y.; et al. *Phys. Chem. Chem. Phys.* **2006**, *8*, 3172−91.
(63) Krylov, A. I.; Gill, P. M. *WIRES: Comput. Mol. Sci.* **2013**, *3*, 317−326.
(64) Dreuw, A.; Weisman, J.; Head-Gordon, M. *J. Chem. Phys.* **2003**, *119*, 2943−2946.
(65) Xue, J.; Rand, B. P.; Uchida, S.; Forrest, S. R. *J. Appl. Phys.* **2005**, *98*, 124903.
(66) Xue, J.; Rand, B. P.; Uchida, S.; Forrest, S. R. *Adv. Mater.* **2005**, *17*, 66−71.
(67) Tang, J. X.; Zhou, Y. C.; Liu, Z. T.; Lee, C. S.; Lee, S. T. *Appl. Phys. Lett.* **2008**, *93*, 043512.
(68) Giebink, N. C.; Lassiter, B. E.; Wiederrecht, G. P.; Wasielewski, M. R.; Forrest, S. R. *Phys. Rev. B* **2010**, *82*, 155306.
(69) Akaike, K.; Kanai, K.; Ouchi, Y.; Seki, K. *Adv. Funct. Mater.* **2010**, *20*, 715−721.
(70) Dutton, G. J.; Robey, S. W. *J. Phys. Chem. C* **2012**, *116*, 19173−19181.
(71) Jailaubekov, A. E.; Willard, A. P.; Tritsch, J. R.; Chan, W.-L.; Sai, N.; Gearba, R.; Kaake, L. G.; Williams, K. J.; Leung, K.; Rossky, P. J.; Zhu, X.-Y. *Nat. Mater.* **2013**, *12*, 66−73.
(72) Lee, M. H.; Dunietz, B. D.; Geva, E. *J. Phys. Chem. Lett.* **2014**, *5*, 3810−3816.
(73) Chai, J.-D.; Martin, H.-G. *J. Chem. Phys.* **2008**, *128*, 084106.
(74) Chai, J.-D.; Martin, H.-G. *Phys. Chem. Chem. Phys.* **2008**, *10*, 6615−6620.
(75) Cossi, M.; Rega, N.; Scalmani, G.; Barone, V. *J. Comput. Chem.* **2003**, *24*, 669−681.
(76) Loutfy, R. O.; Sharp, J. H. *J. Chem. Phys.* **1979**, *71*, 1211.
(77) Sussman, A. *J. Appl. Phys.* **1967**, *38*, 2738.
(78) Fan, F.-R.; Faulkner, L. R. *J. Chem. Phys.* **1978**, *69*, 3334.
(79) Hebard, A. F.; Haddon, R. C.; Fleming, R. M.; Kortan, A. R. *Appl. Phys. Lett.* **1991**, *59*, 2109−2111.
(80) Pevzner, B.; Hebard, A. F.; Dresselhaus, M. S. *Phys. Rev. B* **1997**, *55*, 16439.
(81) Pandey, R.; Gunawan, A. A.; Mkhoyan, K. A.; Holmes, R. J. *Adv. Funct. Mater.* **2012**, *22*, 617−624.
(82) Lee, M. H.; Dunietz, B. D.; Geva, E. *J. Phys. Chem. C* **2013**, *117*, 23391−23401.
(83) Lee, M. H.; Geva, E.; Dunietz, B. D. *J. Phys. Chem. C* **2014**, *118*, 9780−9789.
(84) Manna, A. K.; Dunietz, B. D. *J. Chem. Phys.* **2014**, *141*, 121102.
(85) Smirnov, S. N.; Liddell, P. A.; Vlassiouk, I. V.; Teslja, A.; Kuciauskas, D.; Braun, C. L.; Moore, T.; Gust, D. *J. Phys. Chem. A* **2003**, *107*, 7567−7573.
(86) Baruah, T.; Pederson, M. R. *J. Chem. Phys.* **2006**, *125*, 164706−164710.
(87) Baruah, T.; Pederson, M. R. *J. Chem. Theor. Comput.* **2009**, *5*, 834−843.
(88) Spallanzani, N.; Rozzi, C. A.; Varsano, D.; Baruah, T.; Pederson, M. R.; Manghi, F.; Rubio, A. *J. Phys. Chem. B* **2009**, *113*, 5345−5349.
(89) Cossi, M.; Rega, N.; Scalmani, G.; Barone, V. *J. Comput. Chem.* **2003**, *24*, 669−681.
(90) Lange, A. W.; Herbert, J. M. *J. Phys. Chem. Lett.* **2010**, *1*, 556−561.
(91) Lange, A. W.; Herbert, J. M. *J. Chem. Phys.* **2010**, *133*, 244111.
(92) Manna, A. K.; Desinghu, B.; Cheung, M.; Dunietz, B. D. To be published.

DOI: 10.1021/ct501018n
J. Chem. Theory Comput. XXXX, XXX, XXX−XXX